



City Research Online

City, University of London Institutional Repository

Citation: Tsavdaridis, K. D., Pilbin, C. & Lau, C. K. (2017). FE parametric study of RWS/WUF-B moment connections with elliptically-based beam web openings under monotonic and cyclic loading. *International Journal of Steel Structures*, 17(2), pp. 677-694. doi: 10.1007/s13296-017-6023-7

This is the accepted version of the paper.

This version of the publication may differ from the final published version.

Permanent repository link: <https://openaccess.city.ac.uk/id/eprint/27012/>

Link to published version: <https://doi.org/10.1007/s13296-017-6023-7>

Copyright: City Research Online aims to make research outputs of City, University of London available to a wider audience. Copyright and Moral Rights remain with the author(s) and/or copyright holders. URLs from City Research Online may be freely distributed and linked to.

Reuse: Copies of full items can be used for personal research or study, educational, or not-for-profit purposes without prior permission or charge. Provided that the authors, title and full bibliographic details are credited, a hyperlink and/or URL is given for the original metadata page and the content is not changed in any way.

City Research Online:

<http://openaccess.city.ac.uk/>

publications@city.ac.uk



City Research Online

City, University of London Institutional Repository

Citation: Tsavdaridis, KD ORCID: 0000-0001-8349-3979, Pilbin, C and Lau, CK (2017). FE parametric study of RWS/WUF-B moment connections with elliptically-based beam web openings under monotonic and cyclic loading. *International Journal of Steel Structures*, 17(2), doi: 10.1007/s13296-017-6023-7

This is the draft version of the paper.

This version of the publication may differ from the final published version.

Permanent repository link: <https://openaccess.city.ac.uk/id/eprint/27012/>

Link to published version: <http://dx.doi.org/10.1007/s13296-017-6023-7>

Copyright: City Research Online aims to make research outputs of City, University of London available to a wider audience. Copyright and Moral Rights remain with the author(s) and/or copyright holders. URLs from City Research Online may be freely distributed and linked to.

Reuse: Copies of full items can be used for personal research or study, educational, or not-for-profit purposes without prior permission or charge. Provided that the authors, title and full bibliographic details are credited, a hyperlink and/or URL is given for the original metadata page and the content is not changed in any way.

City Research Online:

<http://openaccess.city.ac.uk/>

publications@city.ac.uk

FE parametric study of RWS/WUF-B moment connections with elliptically-based beam web openings under monotonic and cyclic loading

*Konstantinos Daniel Tsavdaridis, Christopher Pilbin and Chun Kit Lau

¹Institute for Resilient Infrastructure, School of Civil Engineering, University of Leeds, Woodhouse Lane, LS2 9JT, Leeds, UK

ABSTRACT

This paper provides numerical results investigating the behaviour of steel web-perforated beams with different shaped single openings located close to beam-to-column connections under monotonic and cyclic loading. In particular, the beams considered feature circular and patented elliptically-based perforations. Non-standard elliptically-based perforations have been proposed previously and are optimally designed to maximise resistance against Vierendeel moments and web-post buckling under static loads at the ultimate limit state. Comprehensive parametric nonlinear finite element analyses using the commercial FE package ANSYS were conducted. Initially, a FE model of the beam-to-column WUF-B moment connection was developed and calibrated against pertinent experimental results found in the literature. Next, parametric analyses were undertaken to assess the RWS/WUF-B connection regarding strength (moment), deformation (rotation) and column web shear panel zone deformation for different shapes of beam web perforations, hole sizes and their locations. The study concludes that larger web openings are capable of moving the plastic hinge away from the column face and the CJP weld. Also, interstorey drifts can be controlled with the wise use of the beam web opening size, shape, and distance from the face of the column, as suggested in the paper. Following, a step-by-step design process for RWS/WUF-B connection is presented.

**Corresponding Author
Tel.: +44(0)113 343 2299
E-mail: k.tsavdaridis@leeds.ac.uk*

1. Introduction

1.1 Background

Events of extreme loading on structures such as the 1994 Northridge, California and 1995 Kobe, Japan earthquakes have not only led to the loss of life but highlighted structural deficiencies and lack of existing knowledge. It is acceptable that within twenty years significant progress has been done, however along with technological advances further questions arise.

Steel moment resisting frames (MRFs) have traditionally been used in areas susceptible to high seismicity and are greatly dependent on the beam-to-column connection behaviour. In the past, fully welded connections considered to provide the optimum combination of strength, stiffness, and ductility according to codes, were the major factors in the seismic-resistant design of connections (Eurocode 3 and Eurocode 8). Following these devastating earthquakes, numerous studies were conducted by the Federal Emergency Management Agency (FEMA) and the SAC Joint Venture resulting reports beginning with FEMA 350 (2000) and main aim to develop reliable, practical and cost-effective design guidelines, specifications, and standards of practice in order to reduce the seismic hazards of steel structures and provide mitigating measures.

The defective workmanship that led to the poor quality of the Complete Joint Penetration (CJP) welds was first believed to be the only cause for the brittle damage. Test results by SAC Joint Venture on all pre-Northridge connections indicated that an even improved workmanship was in most cases insufficient by itself to achieve reliable performance. This concluded that connections were not well understood, with various unknown factors contributing to their inadequate performance. Pre-Northridge connections had drawbacks mainly related to their geometry with large stress concentrations occurring in the critical zone where the beam joins the column. This phenomenon made them susceptible to fracture in a brittle manner before yielding occurred, while forming a plastic hinge in the beam very close to the connection resulted in low rotational ductility.

Alternative solutions with pre-qualified moment seismic connections are considered (ASCE, 2000 and EC8, 2005) by reinforcing connections, or using a Reduced Beam

Section (RBS) type of connection (Sofias, et al., 2013), in order to achieve the “weak beam-strong column” mechanism which enables the development of an internal plastic hinge within the beam acting as a ductile seismic ‘fuse’ while is attracting high stresses and allowing beam rotations.

In parallel, a lot of research is carried out the last 15 years on the avoidance of disproportionate collapse of steel frames, following the 9/11 event in the Unites States. It is known that beam-to-column connections should first provide sufficient ductility to sustain large rotations in such a case, but further, allow structural members to carry loads in tension to provide alternative load paths in the case of completely damaged members (e.g., column or group of columns). Almost a decade ago, on an attempt to relate the seismic-resistant design with the blast-related progressive collapse resistance, and having considered the effect of further local actions in adverse loading cases, suggested that the ideal plastic rotations should be in the order of 0.07radian or more as required to initiate the catenary action in a structural frame that is under progressive collapse scenario following its flexural design (Hamburger and Whittaker, 2004). Therefore, it is worth to relate the outcomes from the seismic-resistant design of moment connections to the suggestions by the corresponding practices in collapse conditions.

In particular, the General Services Administration (GSA, 2003) and the Department of Defense (DoD, 2005) guidelines outline failure criteria such as rotational capacities, for various types of steel connections under the progressive collapse phenomenon. Researchers (Sadek et al., 2011 and Kim et al., 2012) often claim that beam-to-column connections can possess significant plastic deformation capacity, larger than those stipulated in the guidelines. Other researchers suggest that seismically designed structures are more resistant to progressive collapse conditions (Carino and Lew, 2001; Khandelwal and El-Tawil, 2007; Kim and Kim, 2009). Hence, by designing seismically resistant connections, the structure’s ductility, robustness and ability to perform a catenary action are also inherently enhanced. Moreover, there are similarities to the loading conditions imposed on a structural frame by both an earthquake and a progressive collapse scenario with the instantaneous removal of a structural member leading to a dynamic response (Kim and Park, 2008 and Alashker et al., 2011).

GSA developed further simplified guidelines for the design of such systems which specify that certain elements of the frame should be proportioned with sufficient strength to resist twice the dead and live load anticipated to be present, without exceeding inelastic demand ratios. However, under general collapse design guidelines, structural members are permitted to experience flexural inelasticity based on allowable values proposed in seismic guidelines as the amplified loading occurs for a very short period, while the long-term loading following removal can be simply treated as a static condition.

The current study is focused on earthquake loads, ignoring the axial forces acting on the beam, but it is an attempt to relate the outcome with the necessary suggestions from GSA and DoD guidelines.

1.2 Code Limitations

The maximum allowable rotational limits are presented to highlight the acceptable criteria outlined by some of the aforementioned design codes and guidelines in **Table 1**, including the RBS connections, as suggested by the GSA and DoD (for low and high level of protection - LOP) guidelines with scope to limit the possibility of progressive collapse when using seismic resistant connections. Similarly, FEMA 356 (2000) has published a table with the acceptable criteria for nonlinear procedures on structural steel components of partially and fully restrained moment connections for all performance limit states. These estimates correspond to typical elements in conventional construction that have not been hardened to resist abnormal loading. The codes do not present any acceptable criteria for reduced web section (RWS) connections, but for the well-studied RBS connections. As both of these methods involve weakening the beam section, the RBS criteria will be used to benchmark the rotations attained herein.

Table 1: Maximum allowable connection rotational limits (in radian)

Connection type	FEMA 356	GSA (2003)	DoD (2005)	
			Low LOP	High LOP
Welded beam flange or cover plate	0.031	0.025	0.035	0.025
RBS	0.05	0.035	0.047	0.035

More recently, DoD (2009) is based on similar design codes and guidelines for earthquake and progressive collapse conditions, in particular, those by GSA (2008), ASCE (2007) and DoD (2005). In DoD (2009) is noted that the *“acceptance criteria in ACSE 41 (2007) are based upon cyclic loadings with bending moment only and rotational capacities are often limited because of degradation and premature loss of strength”*. Hence, it is again suggested that the mobilisation of catenary action found in progressive collapse conditions requires extensive plastic rotations, following the flexural design of connections based on their hysteretic performance.

1.3 RWS Connections

The ability of single web openings to enhance the rotational capacity of steel connections has been recently studied (Hedayat and Celikag, 2009; Yang et al., 2009; Prinz and Richards, 2009; Kazemi and Hosseinzadeh, 2011; Tsavdaridis, 2014; Tsavdaridis et al., 2014; Tsavdaridis and Papadopoulos, 2016). However, the evaluation of such connections under seismic conditions and the relation to progressive collapse limitations has yet to be established.

In parallel, single and multiple web perforations of steel beams of standard and non-standard shapes are widely used in structural steel design due to their ability to provide lighter structural members with reduced material cost, in addition to their allowance for greater flexibility in structural layouts particularly in the floor-to-ceiling height and with longer spans, fewer columns, and foundations. To enhance the structural behaviour of perforated beams, Tsavdaridis and D’Mello (2011, 2012a) developed a newly-patented non-standard web opening configuration which was found to be more effective than the standard traditionally used opening shapes (i.e., circular, hexagonal, square, and elongated) regarding strength and deflections.

The current research study takes advantage of pioneering construction methods used in the steel industry, and presents an investigation into the welded unreinforced flange-bolted web (WUF-B) single-sided seismic moment connections by means of a FE parametric study to provide knowledge on the ability of employing such perforated

beams with scope to enhance their moment and rotational capacity when subjected to monotonic and cyclic loads.

2. Validation of the FE Model

2.1 Introduction

To accurately model the behaviour of the WUF-B single sided moment connection, often referred to as a Pre-Northridge connection, a validation study was initially performed. The FE model was developed based on previous research conducted by Kim et al. (2012) on the performance of similar steel connections but without perforations under cyclic loading. A three-dimensional (3D) FE model was developed using the commercial package ANSYS v.14. A nonlinear (geometric and material) model was carried out and compared with both the experimental and the FE model found by Kim et al. (2012). The experimental apparatus and the test specimen are shown in **Figure 1**.

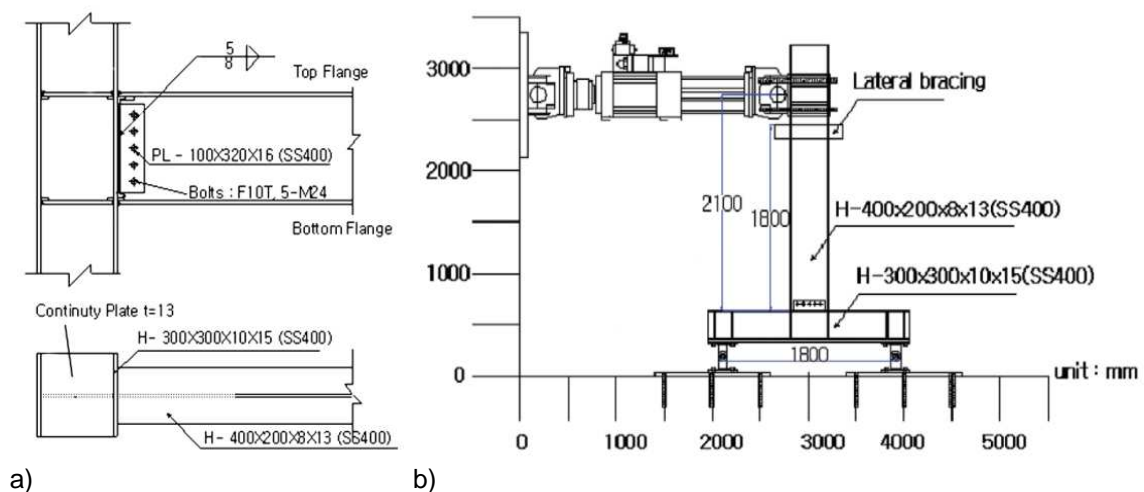


Figure 1: a) Connection properties; b) Experimental setup (adopted by Kim et al., 2012)

The 3D FE model was consisted of shell elements S4R; a 4-node reduced integration element with displacement and rotational degrees of freedom (**Figure 2**). Five M24 fasteners were used to connect the shear tab (fin plate) to the beam web. The connection type was selected as a rigid 'beam element' with a physical radius of 12mm to simulate the link projected between the two surfaces. The rigid elements allow rotations but do not fail under significant extension, since the actual contact interface between the shear tab and the beam web cannot be modelled. In such way, stresses can be mobilised from the column web shear panel zone to the CJP welds and in the vicinity

of the beam web opening, ensuring that there is not bolt failure. In common, RBS and RWS connections always reach their ultimate moment capacities before fracture in the material is initiated. Hence, the simplification of the FE model will not impact the results while conclusions will be based on comparing the maximum capacities of the connections with different geometries of web openings.

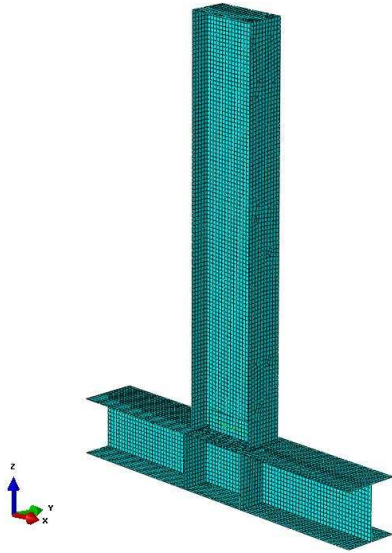


Figure 2: Modelled connection assembly with 3D shell elements

2.2 Material Properties

A bilinear stress-strain relationship was used to model the nonlinear behaviour of the assembly. For the linear elastic response of the beam and column, a Young’s modulus, $E=190\text{GPa}$, and Poisson’s ratio, $\nu=0.3$, were used together with the Von Mises yield criterion employed. The actual material properties of the assembly components were taken from the coupon test measurements for the yield, and ultimate strengths and they are summarised in **Table 2**.

Table 2: Connection assembly coupon material properties

Member	Component	Yield Strength, f_y [MPa]	Ultimate Strength, f_u [MPa]
Beam	Flange	281	423
	Web	332	438
Column	Flange	281	433
	Web	304	450

The isotropic hardening material model was assumed for the assembly under monotonic loading, and kinematic hardening under cyclic loading, similarly to Mao et al., 2001; Ricles et al., 2003; Hedayat and Celikoglu, 2009, as they are investigating the seismic performance of similar connections.

2.3 Loading Protocol Adopted and Analysis Results

The assembly was then loaded under monotonic and cyclic loading sequences. For the monotonic loading, a displacement was applied to the beam's tip to replicate the force imposed by the actuator in the experimental set-up. Cyclic loading was performed using the SAC loading protocol outlined by FEMA 350 (2000), using beam-end displacements for 32 cycles, as shown in **Figure 3**.

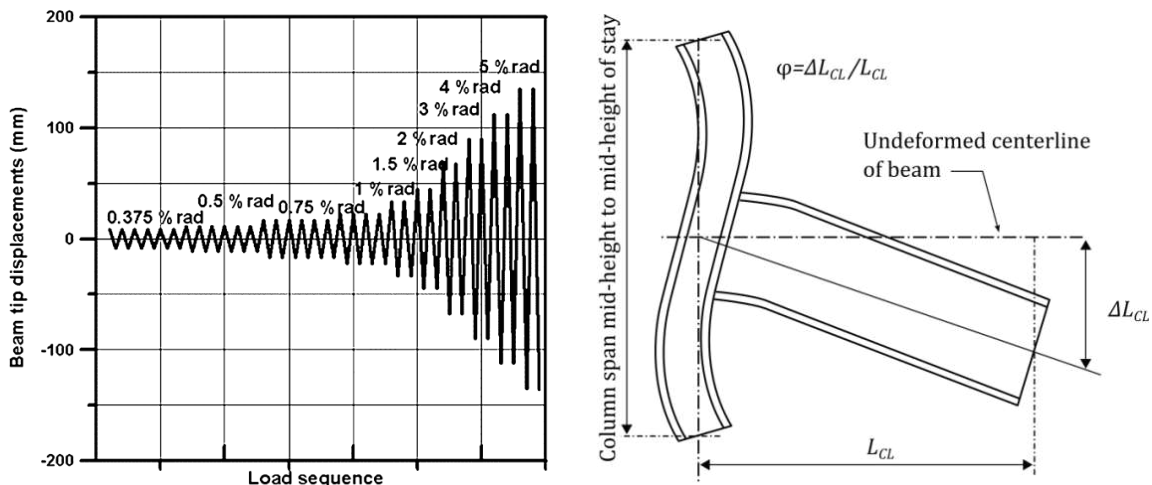


Figure 3: (a) Cyclic loading sequence (adopted by Kim et al., 2012) and (b) Angular rotation of test assembly

An Eigen buckling analysis was initially reformed to derive the first Eigen mode shape, hence, introduce small imperfections, which were then used, after being scaled by the recommended factor of $t_w/200=8200=0.04\text{mm}$, to update the geometry. Next, the nonlinear (geometric and material) analysis was performed with the full 64 load-steps using the "Newton-Raphson" approach.

2.4 Results

A comparison between the experimental and FE models is illustrated in **Figures 4** and **5** for both loading sequences. The maximum normalised moment acquired from the experimental test and the FE analysis developed in the literature was 1.070 and 1.096, respectively. The maximum normalised moment recorded from the FE model developed in the current study was 1.169, corresponding to a percentage error of 8.8% compared to the experimental test and 6.2% to the FE analysis. Overall, there is a satisfactory correlation between the results illustrated in the graphs with both FE models presenting slightly stiffer responses when compared to the experimental model. The initial stiffness is in the perfect agreement between the two FE analyses.

It is observed that the moment capacities recorded from the experimental model under cyclic loading were somewhat higher due to the modelling simplifications. However, the scope of the study was to observe and compare the stress distribution in the vicinity of the web opening while using different web opening configurations, without considering the stress condition of the bolts and assuming that they have the necessary capacity to transfer the stresses to the beam.

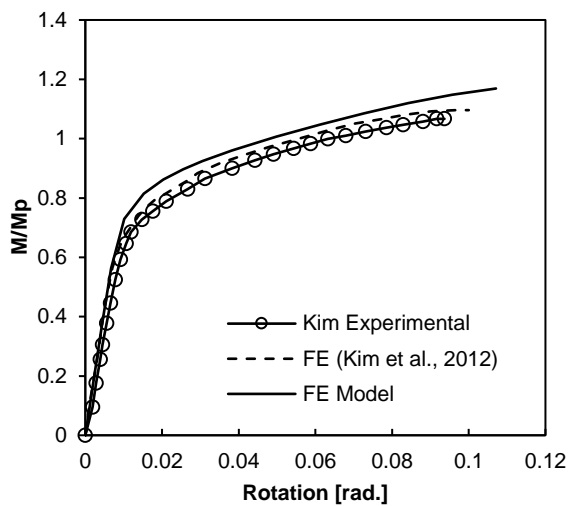


Figure 4: Comparison of monotonic loading responses

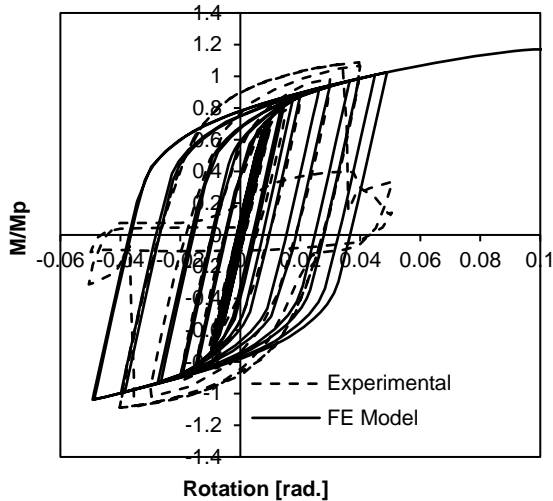


Figure 5: Comparison of cyclic loading responses

3. Parametric Study and Numerical Results

3.1 Parametric Models

The WUF-B connection depicted in **Figure 7** with a single perforation in the web of the beam is examined herein and compared to the same connection while using a beam with a standard circular web opening as well as a solid webbed beam. The elliptically-based web openings, first introduced by Tsavdaridis and D’Mello (2011), are formed by straight lines to ease the fabrication process (**Figure 6**) and semi-circles to avoid stress concentrations at the critical areas (i.e., top and bottom tee-sections). Compared to the traditional circular, and hexagonal web openings, perforated beams with such mixed-0shaped web openings have shown to be more efficient on local beam deflections, moment capacities, and stress distribution under static load conditions.

The geometric parameters that define these elliptically-based web opening shapes are the opening depth, d_o , the angle of the straight-edge lines, θ , and the semi-circle radius, R . Two web openings are examined in this study as opening A (with $R=0.30d_o$ and $\theta=30^\circ$) and opening B (with $R=0.15d_o$ and $\theta=10^\circ$). For the direct comparison, the circular web opening C is also assessed.

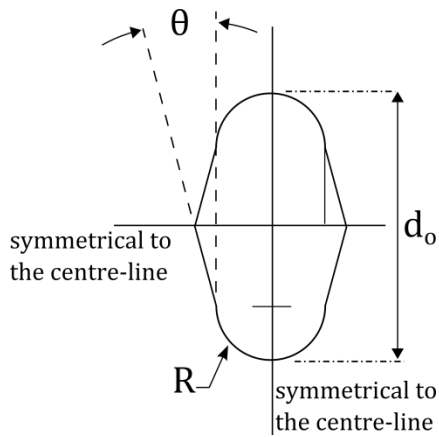


Figure 6: Geometric parameters of web openings (Tsavdaridis and D’Mello, 2011)

3.2 Parametric Variables

The geometric parameters for investigation are considering the effect of the opening depth, d_o , and the distance from the column face to the web opening centreline, S . Three options were selected for each case, and they are dependent on the beam height, h , as follows:

- $d_o = 0.5h; 0.65h; 0.8h$
- $S = 0.87h; 1.3h; 1.7h$

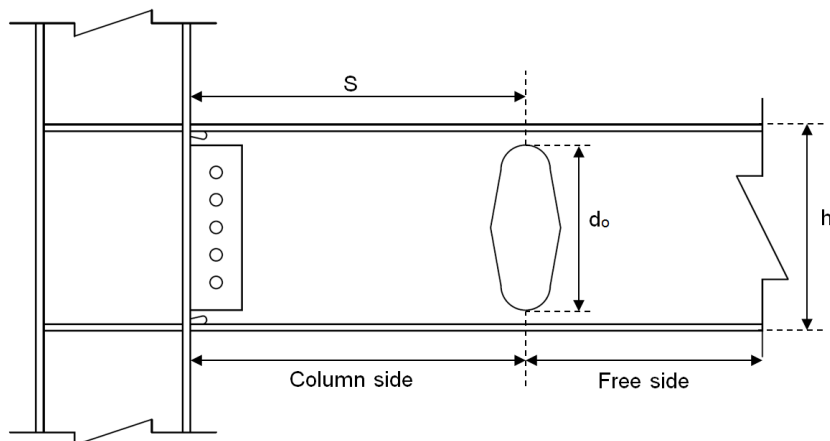


Figure 7: WUF-B connection model and web opening geometric parameters

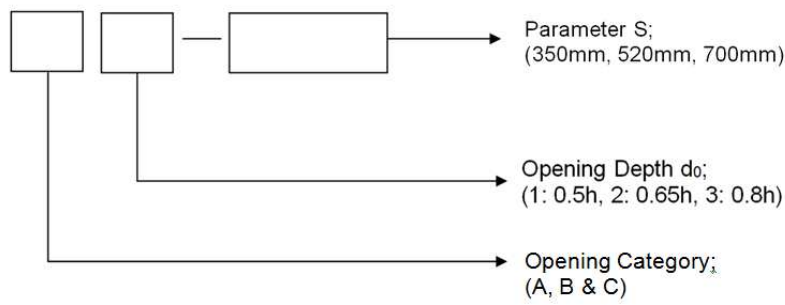


Figure 8: Classification reference of the connection model

The connection models are categorised as illustrated in **Figure 8**. For example, an RWS/WUF-B connection with a web opening A and a depth of 0.65h (260mm), located 700mm from the face of the column, would correspond to the classification A2-700. In total, 27 models are analysed and discussed.

Table 3: Summary of results for various RWS/WUF-B connections

CONNECTION MODEL	Web Opening Area [mm ²]	MONOTONIC				CYCLIC		Monotonic/ Cyclic
		Ultimate moment, M_u [kNm]	Ultimate rotation, ϕ_u [rad.]	Panel Zone		Ultimate moment, M_u [kNm]	Ultimate rotation, ϕ_u [rad.]	
				Rotation at max. Panel zone defl., [rad.]	Max. Panel zone defl., [mm]			
Solid	0	468.5	0.1290	0.2320	20.17	391.7	0.0497	2.60
A1-350	22758	442.7	0.1163	0.1260	14.58	390.4	0.0499	2.33
A1-520	22758	462.5	0.1262	0.1850	17.57	390.5	0.0499	2.53
A1-700	22758	467.5	0.1279	0.2170	18.44	390.7	0.0500	2.56
A2-350	38457	390.0	0.0775	0.0790	9.16	385.5	0.0496	1.56
A2-520	38457	425.1	0.0943	0.0960	12.36	389.7	0.0499	1.89
A2-700	38457	454.9	0.1180	0.1180	13.96	389.5	0.0499	2.36
A3-350	58259	304.0	0.0231	0.0240	1.70	331.7	0.0499	0.46
A3-520	58259	322.5	0.0293	0.0290	2.41	320.8	0.0499	0.59
A3-700	58259	339.0	0.0368	0.0620	3.34	335.8	0.0499	0.74
B1-350	12949	447.2	0.1112	0.1200	15.23	390.6	0.0498	2.23
B1-520	12949	466.5	0.1277	0.1980	17.40	390.5	0.0499	2.56
B1-700	12949	467.8	0.1292	0.2190	18.50	390.4	0.0499	2.57
B2-350	21895	416.4	0.0940	0.0970	11.27	389.2	0.0499	1.88
B2-520	21895	442.3	0.1082	0.1080	14.34	390.1	0.0499	2.17
B2-700	21895	466.8	0.1280	0.1370	17.82	390.0	0.0498	2.57
B3-350	35062	350.4	0.0386	0.0390	4.17	347.4	0.0499	0.77
B3-520	35062	375.2	0.0542	0.0560	6.05	371.5	0.0497	1.09

B3-700	35062	401.2	0.0743	0.0740	9.48	384.9	0.0499	1.49
C1-350	31410	431.7	0.1087	0.1110	12.99	382.0	0.0487	2.23
C1-520	31410	454.9	0.1234	0.1699	16.89	382.7	0.0493	2.50
C1-700	31410	458.6	0.1254	0.1466	19.99	389.7	0.0498	2.52
C2-350	53083	375.7	0.0537	0.0577	6.41	369.5	0.0495	1.08
C2-520	53083	399.0	0.0710	0.0710	9.16	380.9	0.0497	1.43
C2-700	53083	429.2	0.0951	0.1032	13.03	384.8	0.0479	1.98
C3-350	80410	263.7	0.0184	0.0192	0.77	260.8	0.0187	0.98
C3-520	80410	277.5	0.0220	0.0220	1.00	275.5	0.0198	1.11
C3-700	80410	298.3	0.0257	0.0257	1.49	295.1	0.0249	1.04

3.3 FE Analysis

A simplified approach was used for the material properties of the FE model, and all components of the connection are of steel grade S500 to provide material uniformity across the beam, column, plates, bolts, and welds. This theoretical approach was followed to support the investigation on the stress concentration areas and to understand further the hierarchy of the failure mechanism. The boundary conditions were applied similarly to the model used in the validation study. The beam's tip was loaded both monotonically and cyclically, and a summary of the results recorded is presented in **Table 3**.

3.4 Beam Failure Mechanism

The transfer of shear forces in the vicinity of the web opening induces local bending moments, known as Vierendeel mechanism. The development of the Vierendeel mechanism around the openings is linked to the formation of four plastic hinges at certain angles about the centreline of the opening. The dominant parameter which affects the Vierendeel mechanism is the critical opening length that varies dependent on the particular web opening shape. Traditional web opening shapes tend to have large critical length, with the worse being the elongated web openings, then the circular openings, and with the most favourable the hexagonal openings where all four plastic hinges are concentrated at the sharp-corner edge points. It is important that with the use of circular web openings, the actual position of the plastic hinges and hence the actual critical opening length cannot be predicted due to the smooth curvy edge. On the other hand, the use of vertical elliptically-based web openings identifies the position of

the plastic hinges and promotes narrow critical opening length, thus robust smaller local deflections which take place at higher loads.

Figure 9 presents the development of plastic hinges for the same sized opening ($d_o=0.8h$) at different distances from the column face. It is observed that the beam with opening B develops the plastic hinges similarly to the beam with opening A when at the same distance S (700mm).

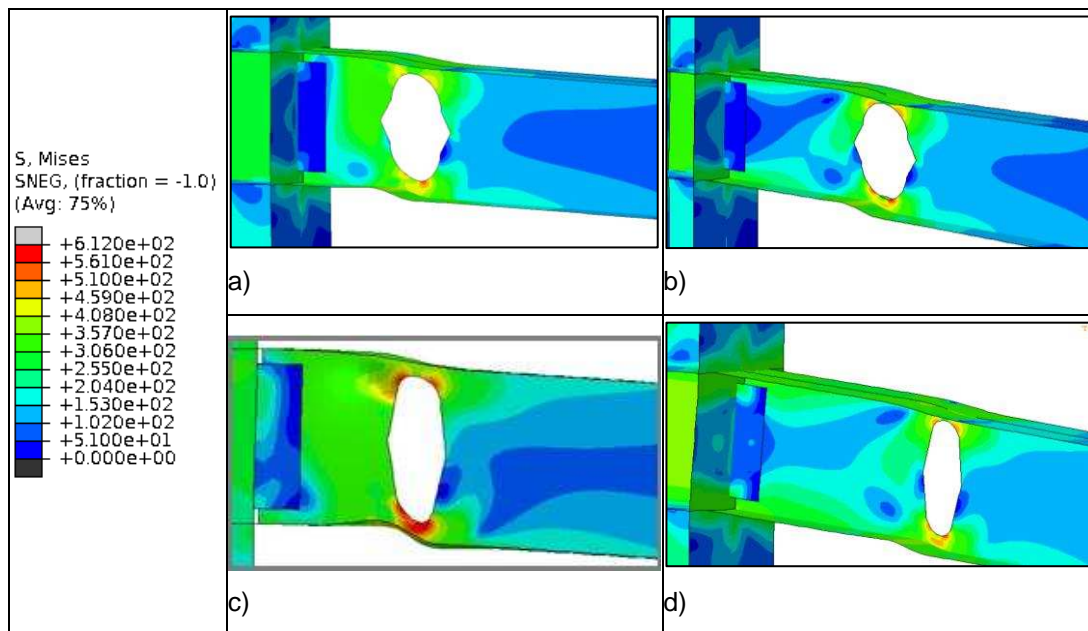


Figure 9: Von Mises stress distribution and Vierendeel mechanism a) A3-350; b) A3-700; c) B3-350; d) B3-700

Plastic hinges were not formed in beams with small web openings, despite the weakened web, as it still can resist global shear stresses. As a result, high stresses are developed in the column web shear panel zone and on the shear tab of the RWS/WUF-B connection as the beam rotates. Deformation of the top and bottom flanges occurred when large openings were used while local Vierendeel mechanism was developed, with lower stresses to be found in the panel zone and the shear tab.

3.5 Stress Concentration in the Connection Components

High stresses around CJP weld, particularly in the top flange, increase the possibility of brittle failure in the connection, presented as brittle fracture occurred because of the

high tri-axial stress-state in the CJP weld region that can induce micro-cracking and trigger rapid crack propagation.

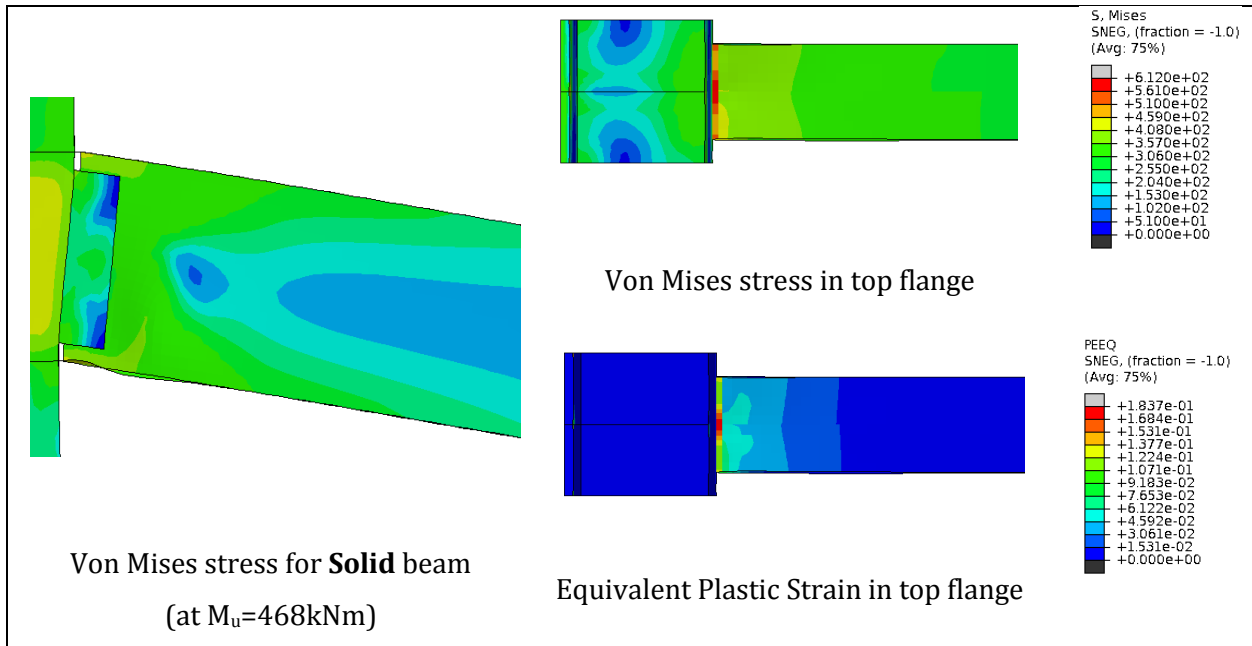


Figure 10: Stress and strain distribution for solid webbed beam

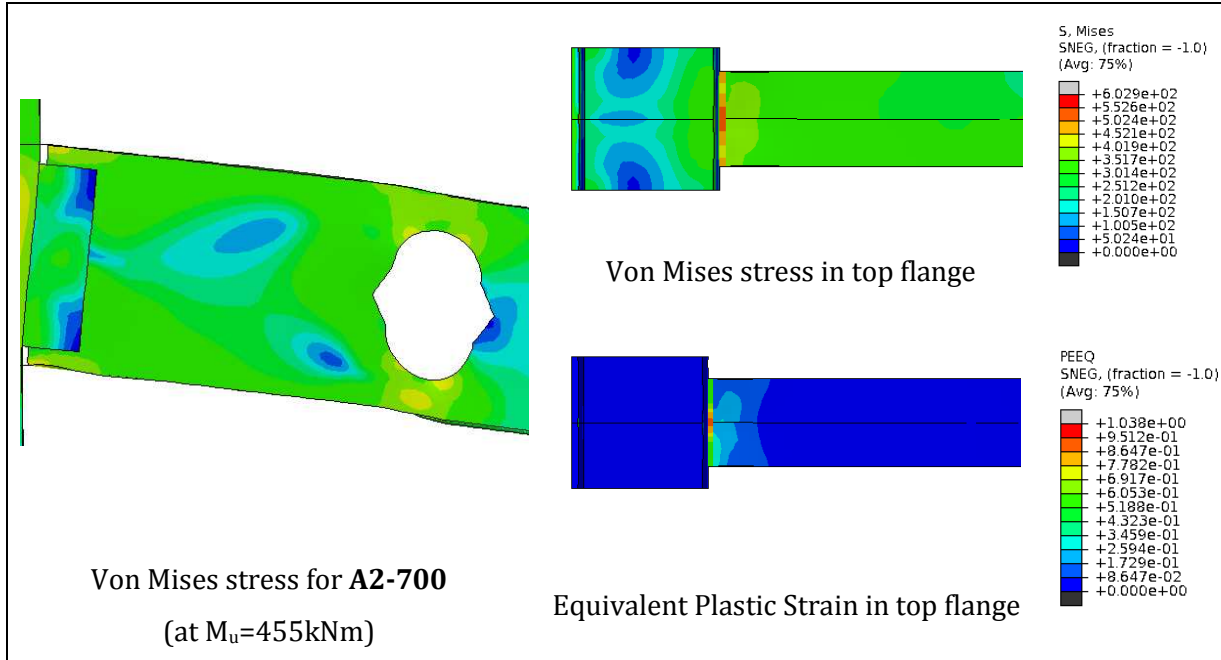


Figure 11: Stress and strain distribution for opening A2-700

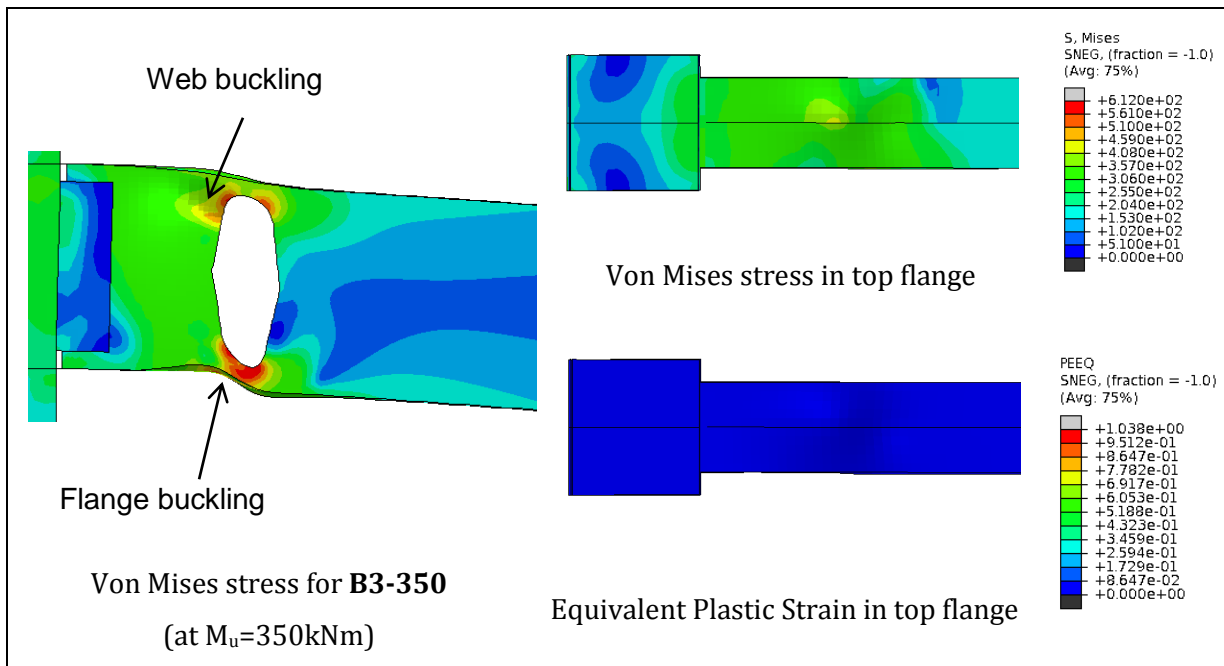


Figure 12: Stress and strain distribution for opening B3-350

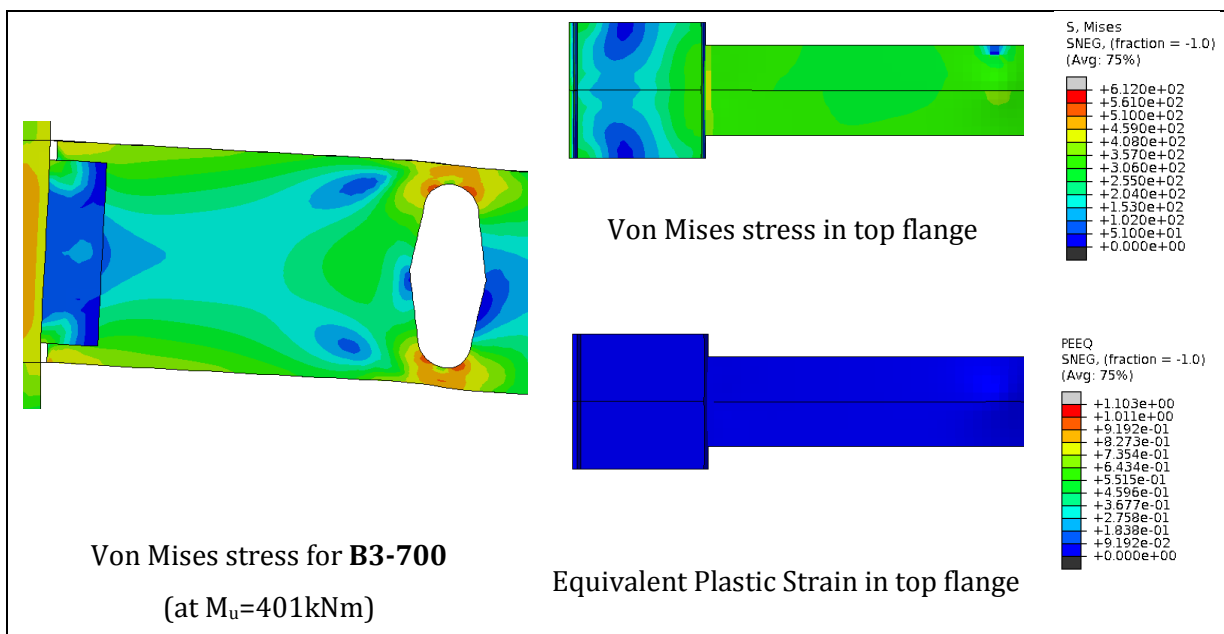


Figure 13: Stress and strain distribution for opening B3-700

RWS/WUF-B connections with large openings ($d_o=0.8h$) were found to be the most effective in mobilising the stress from the top flange CJP weld way from the column face due to the development of the Vierendeel mechanism in the perforated beam. **Figures 10 to 13** depict the plastic in the vicinity of the web openings. When the web opening is placed closer to the face of the column ($S=350\text{mm}$), the connection undergoes higher shear forces as the opening is in proximity to the shear tab and column face. This results

in the large deflection of the beam flanges as demonstrated in **Figure 12**. Consequently, the use of large web openings enables the desirable ductility of the connection at the cost of a reduced strength connection.

Excessive buckling of the beam web and flange in the vicinity of large web openings was observed when the connection subjected to cyclic loading (**Figure 14**). When hogging moment applied, tension was experienced in the top flange of the beam and significant buckling in the bottom flange.

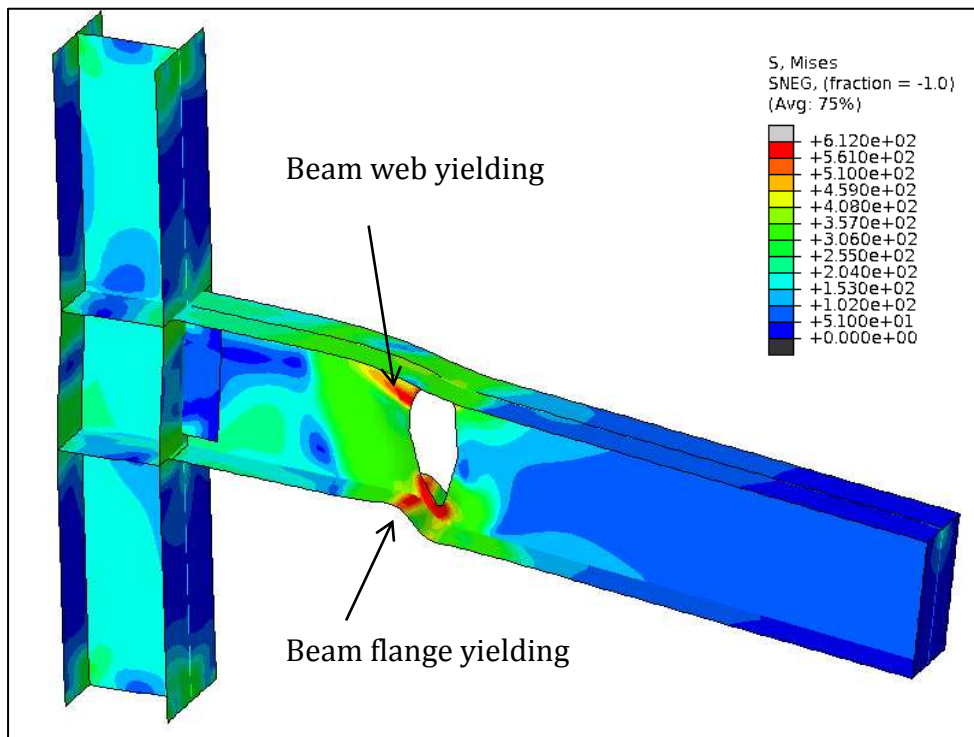


Figure 14: Vierendeel failure mode for B3-700

On the other hand, when beams with small web openings are used, no difference in the stress-state around the weld was observed. In fact, high stresses were found on the top flange CJP weld in a similar fashion to the connections using solid webbed beams (**Figure 10**). This suggests that RWS/WUF-B connections with small openings might fail by brittle fracture. Consequently, it was concluded that RWS/WUF-B connections using perforated beams with single small web openings of any shape are not influenced by the change in their distance from the column face, and current general rules can be applied to the design of the connection. Also, little differences between opening A and B were

captured while the stress distribution largely dependent on the d_o , and S , for large web openings.

4 Results: Monotonic Loading

4.1 Connection Strength

The strength of the connection is determined by its ultimate moment capacity while following that the moment capacity was decreased while the rotation still increases. As it was anticipated, the connection with the solid webbed beam carries the highest load ($M_u=468.5\text{kNm}$). Connections with small web opening areas (i.e. A1, B1, and C1) present almost identical moment-rotation behaviour to the solid webbed beam. This suggests that smaller openings do not influence the overall response of the connection.

Figure 15 illustrates the ultimate moment recorded against the web opening area, and the effect of distance, S . It becomes apparent that as the area of the opening increases, the ultimate moment of the connection reduces. Connections using perforated beams with large openings ($d_o=0.8h$) are less influenced by the parameter S , whereas connections with smaller openings are indeed affected. For example, reducing the web opening size from $0.65h$ (A2) to $0.5h$ (A1) had almost no effect on the connection's strength when S is equal to 700mm (**Figure 15c**). Openings positioned near the column face experience greater shear stresses in the shear tab and flange CJP welds. Hence, the deflection of the flanges is initiated at a lower loading level. Another example is demonstrated with connections using perforated beams with opening B (narrow elliptical with the smallest web opening area), which have higher moment capacities when compared with connections using openings A and C, despite the depth of the opening (i.e., the maximum reduced cross-section dimension). The RWS/WUF-B connection with the highest capacity is the B1-700, and the weakest one is the A3-350 amongst all studied models, with a difference in moment capacity of 35.1%.

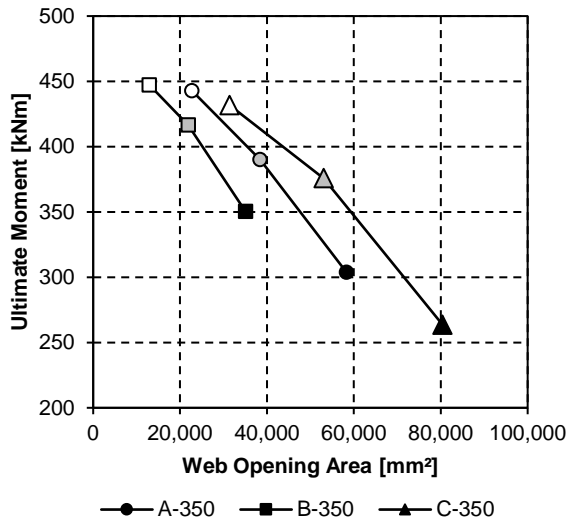


Figure 15a: Effect of web opening area on strength of connection for S=350mm

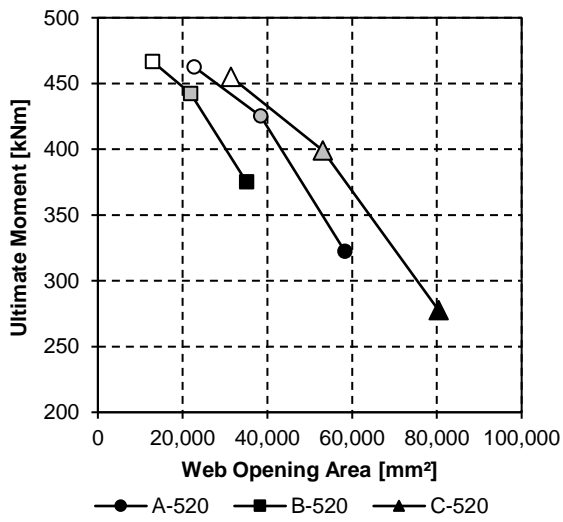


Figure 15b: Effect of web opening area on strength of connection for S=520mm

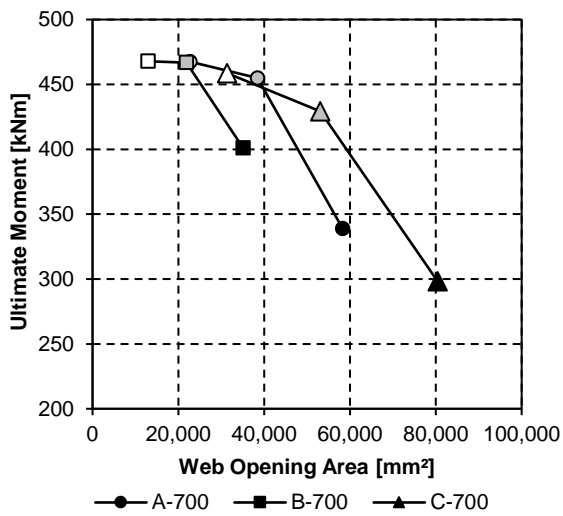


Figure 15c: Effect of web opening area on strength of connection for S=700mm

The results establish that placing smaller openings even close to the column face does not greatly alter the strength of the connection. It could be then suggested that perforated beams with small and medium single web openings could be used in moment resisting steel frames without compromising the strength of the connection.

4.2 Rotational Capacity

The ultimate rotation corresponding to the ultimate moment capacity of the connection was recorded from the centreline of the column. Due to the presence of the opening, the overall rotation is also affected by the local deformations at the low and high moment sides of the opening with the top and bottom tee-sections being deflected due to the Vierendeel mechanism (**Figure 16**). It was observed that the local deformation was increased when the opening was located further away from the face of the column.

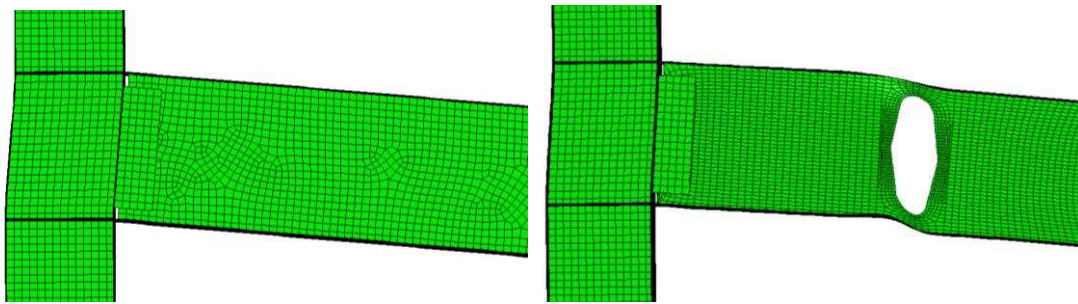


Figure 16: Rotated connection models using solid webbed and perforated beam

Figure 17 illustrates the ultimate rotation recorded about the web opening area, and the effect of distance, S .

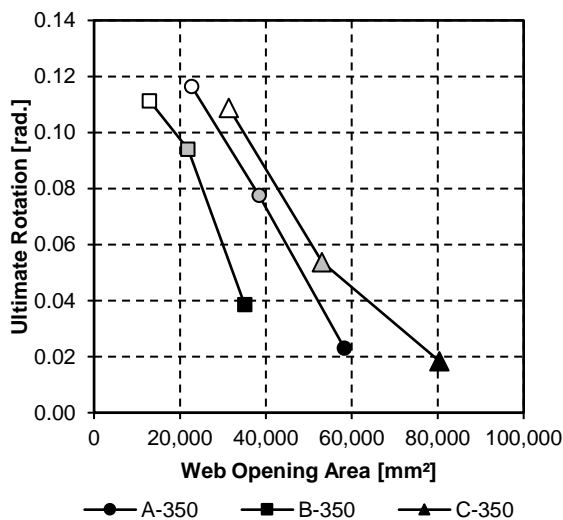


Figure 17a: Ultimate rotation of openings for $S=350\text{mm}$

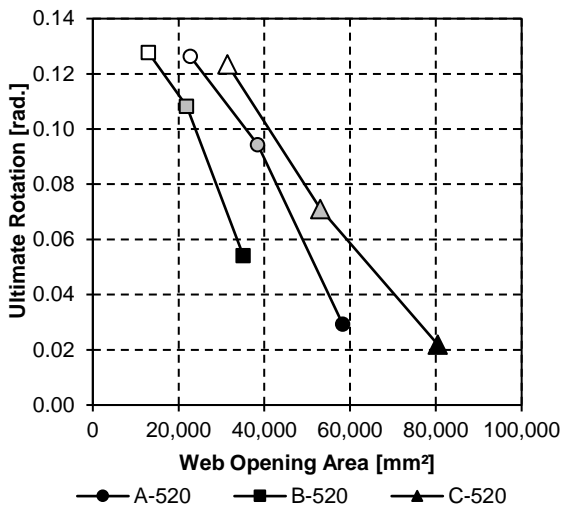


Figure 17b: Ultimate rotation of openings for S=520mm

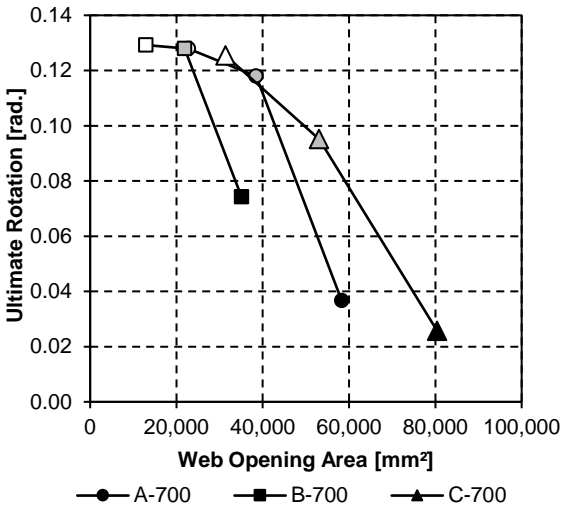


Figure 17c: Ultimate rotation of openings for S=700mm

In general, higher rotational capacities were attained by the RWS/WUF-B connections using perforated beams with the narrowest elliptically-based web opening B, compared to the opening A and circular opening C, for the same opening depth (d_o), due to the smaller critical opening length, which is the main parameter that triggers the local Vierendeel mechanism (Tsavdaridis and D’Mello, 2012a). Connections with medium ($d_o=0.65h$) and large ($d_o=0.8h$) size web openings experience low rotational capacity under monotonic loading independent of the distance, S.

5 Results: Cyclic Loading

5.1 Connection Strength

Similarly to the validation study, the connections were loaded under 32-cycles according to the SAC protocol. Under cyclic loading conditions, the connections' moment capacities followed a similar trend to those illustrated under monotonic loading. The connection with the solid webbed beam was again the strongest ($M_u=391.7\text{kNm}$), but lower compared to the one recorded in the monotonic loading study.

From **Figure 18**, it is found that the ultimate moment capacities of the connections about the web opening areas recorded from the cyclic loading test demonstrate a different trend in contrast to the more 'linear' trend observed when the models subjected to monotonic loading. This is a result of the strength degradation that connections experience under cyclic loading. It is worth to note that the RWS/WUF-B connections with small ($d_o=0.5h$) and medium ($d_o=0.65h$) size openings behave similarly, as opposed to the ones with large web openings in which a significant decrease of moment capacity was recorded. In more detail, the greater is the critical opening length, c , the higher is the cyclic degradation that the connection experiences due to the Vierendeel mechanism.

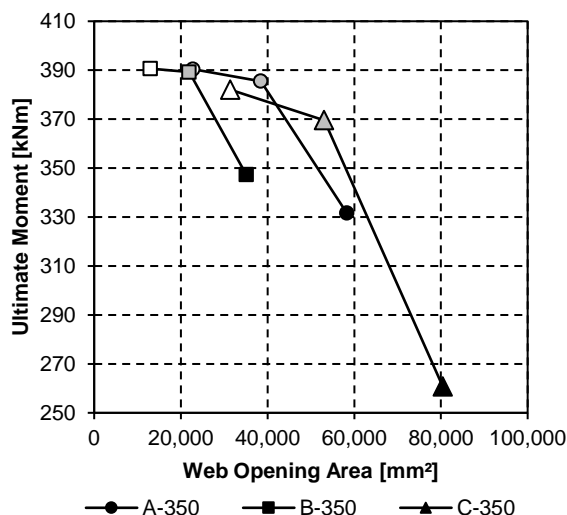


Figure 18a: Effect of web opening area on strength of connection for $S=350\text{mm}$

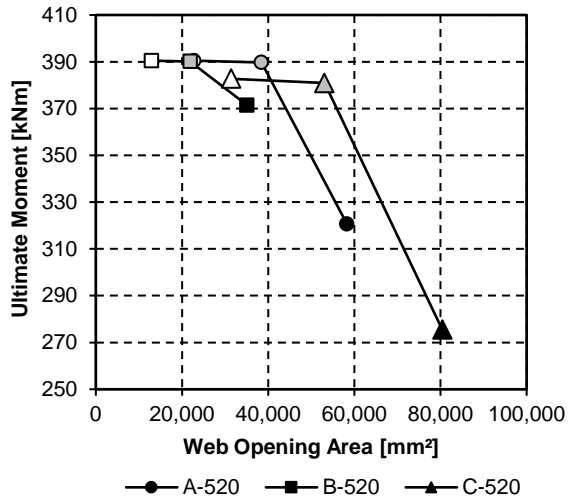


Figure 18b: Effect of web opening area on strength of connection for **S=520mm**

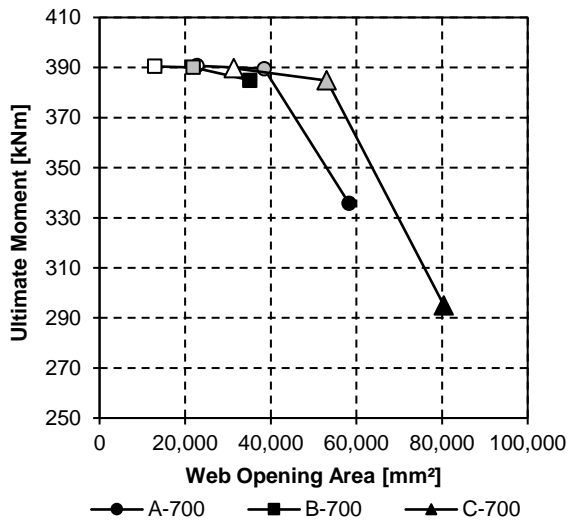


Figure 18c: Effect of web opening area on strength of connection for **S=700mm**

5.2 Rotational Capacity

The rotational capacities of RWS/WUF-B connections subjected to cyclic loading are limited due to degradation and premature loss of strength. This is prominent for connections using perforated beams with large openings ($d_o=0.8h$), as it is depicted by the hysteric behaviour in **Figure 19**.

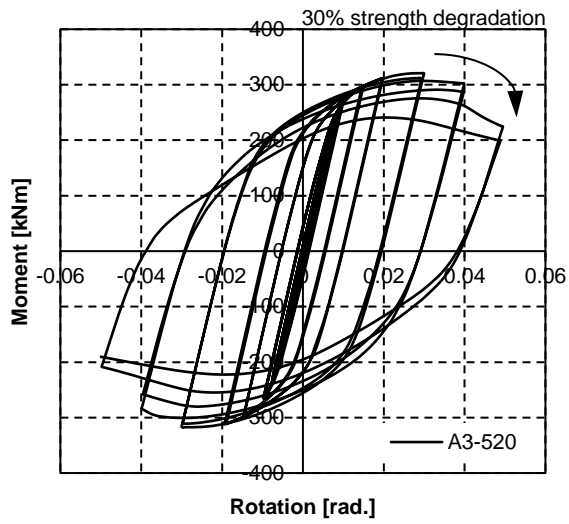


Figure 19a: Hysteretic behaviour of opening A3-520

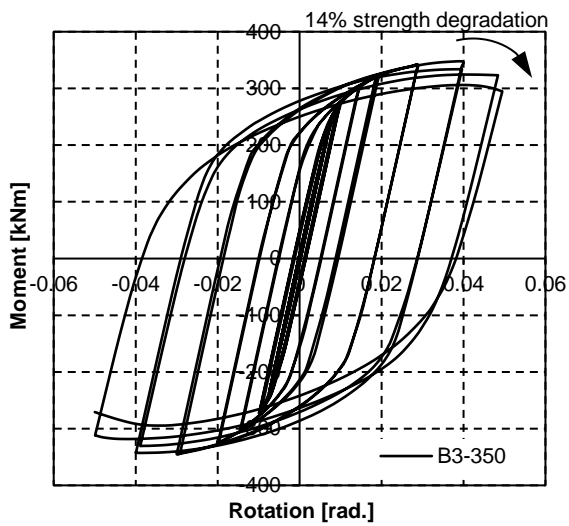


Figure 19b: Hysteretic behaviour of opening B3-350

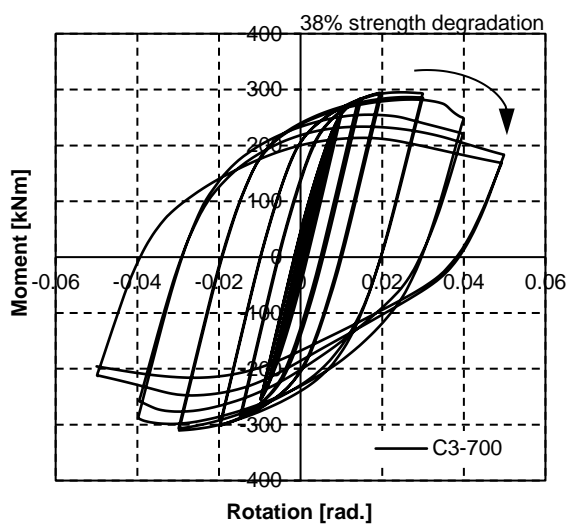


Figure 19c: Hysteretic behaviour of opening C3-700

All connection models illustrated very similar ultimate rotational capacities with the only difference found for connections using the largest traditional circular opening, C3. The connections with the new combine-shapes web openings were able to achieve full ultimate rotational capacity similar to the connection using solid webbed beam, while the panel zone deflection is expected to be significantly reduced and high stresses mobilised away of the connection's components.

6 Panel Zone Shear Deformation under Monotonic Loading

It is important to reduce the interstory drifts and the panel zone deformation during seismic and collapse conditions. The deformation of the panel zone was recorded under monotonic loading to determine the effect of the opening to the initial stiffness of the connection, and it was measured as a relative deflection from the centreline of the column. The shear deformation also contributes to localised bending stresses which lead to the fracture of the top flange CJP weld. The resistance capacity was acquired by both the column web and the continuity plates (i.e. stiffeners) between the column flanges. The energy dissipated in the connection was absorbed in the panel zone region when the maximum moment was achieved before any local buckling occurred in the beam flanges or the web.

RWS/WUF-B connections are found effective in reducing the shear deformation of the panel zone, due to the development of plastic hinges in the vicinity of the openings (**Figure 20**). The maximum panel zone deflection is obtained for the connection with the solid webbed beam and it is equal to 20.17mm (**Table 3**). In particular, when the distance, S , was equal to 350mm or 520mm, the change in shear deformation of the panel zone for all opening types is almost directly proportional to the web opening area.

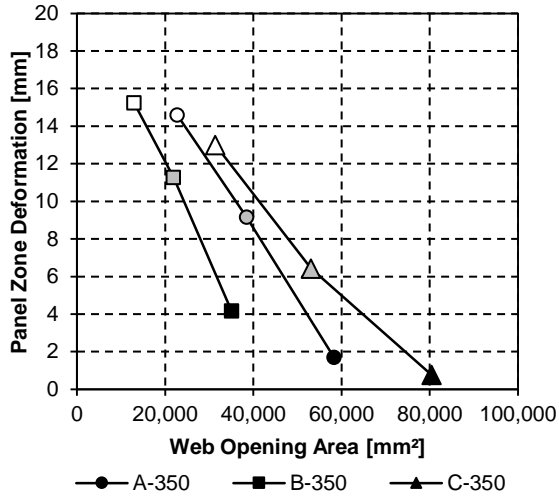


Figure 20a: Panel-zone shear deformation when S=350mm

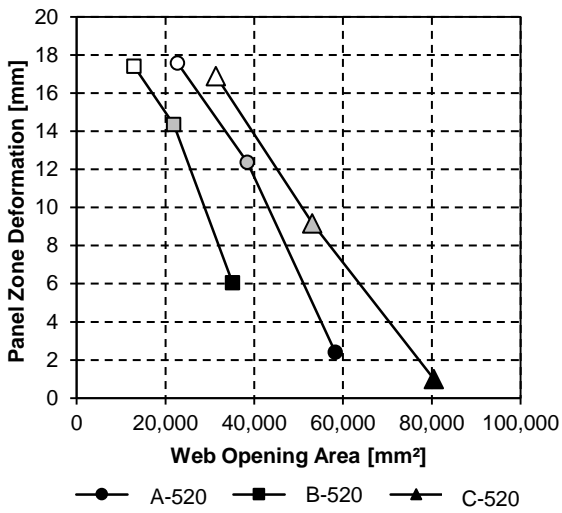


Figure 20b: Panel-zone shear deformation when S=520mm

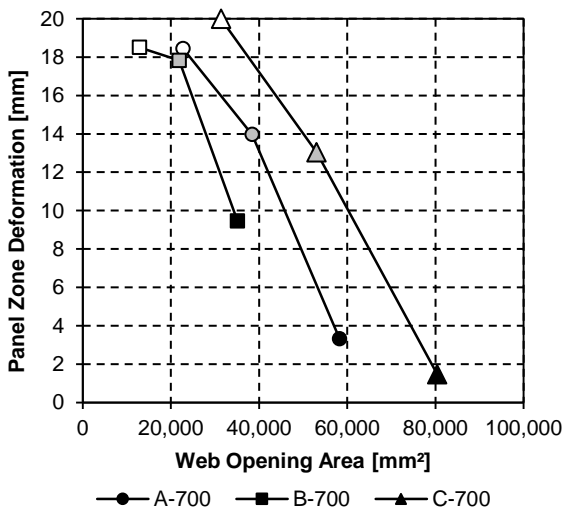


Figure 20c: Panel-zone shear deformation when S=700mm

The use of large web openings ($d_o=0.8h$) reduced significantly the deformation of the panel zone; this is highlighted by the use of perforated beams and the opening type A and C, as they promote local beam deflections and buckling in the vicinity of the reduced section. Oppositely, high deformation of the panel zone was resulted when small web openings were used in combination with the distance S equal to 700mm. For instance, the RWS/WUF-B connection with the perforated beam using the opening type C and distance, S , equal to 700mm, resulting in critical high panel zone deformation similar to the connection with the solid webbed beam.

7 Rotational Moment Capacity of RWS/WUF-B Connections

The rotational moment capacity of the RWS/WUF-B connection is dependent on:

- 1. Vierendeel bending at reduced web section in rotation (section 7.1)**
2. Column bending in rotation (EC3, 2005 and P358, 2014)
3. Bolt bearing failure in fin plate in rotation (EC3, 2005 and P358, 2014)
- 4. Yielding of shear tab (fin plate) in rotation (section 7.2)**
5. Yielding of beam web in rotation (EC3, 2005 and P358, 2014)

The design process of RWB/WUF-B connection is synopsised in the following flow chart:

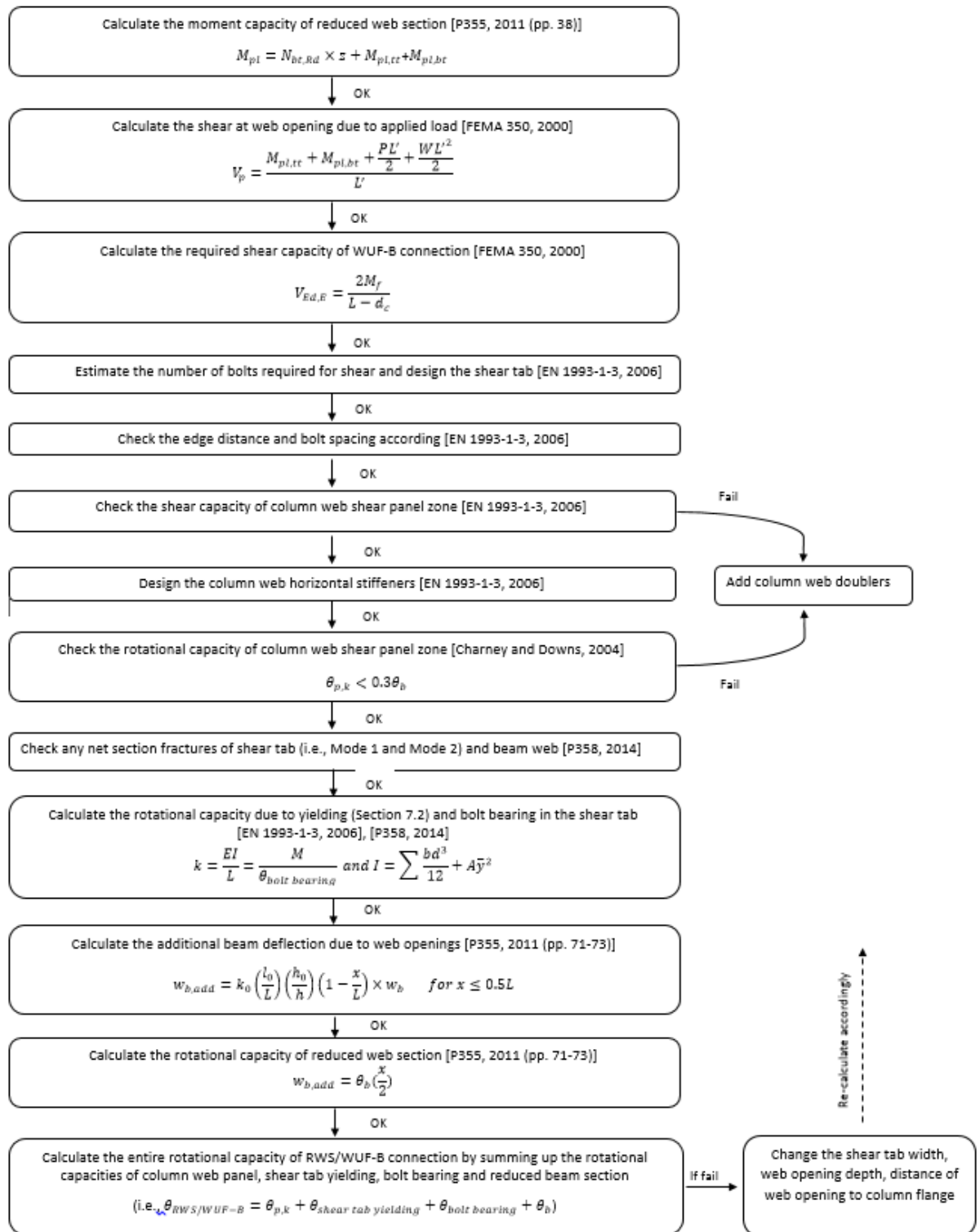


Figure 21: Design process of RWS/WUF-B connections

This analytical study will be focused on the yielding of fin plates and the Vierendeel bending at the reduced web section of the beam. EC3 (2005) and the P358 (2014) includes the calculation of the moment capacity due to yielding of beam web, bending of column and bolt bearing failure in fin plate.

7.1 Vierendeel Bending at Reduced Beam Web Section

The moment capacity of the reduced web section is comprised of the coupled Vierendeel moment and moment due to axial forces in top and bottom tee-sections, while there is compression at top tee-section and tension at bottom tee-section. The Vierendeel moment (i.e., M_{t1} and M_{b1} OR $M_{pl,tt}$ and $M_{pl,bt}$) is formed due to the local bending actions (Tsavdaridis and D'Mello, 2012b).

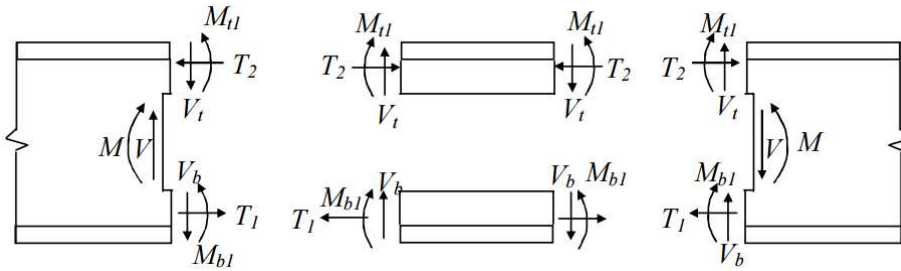


Figure 22: Shear and moment interaction at reduced web section (Narayanan et al., 1999)

The moment capacity of the reduced web section is calculated by:

$$M_{pl} = N_{bt,Rd} \times z + M_{t1} + M_{b1}$$

The tensile resistance of top or bottom tee-section are calculated by:

$$N_{bt,Rd} = \frac{A_{bt}f_y}{\gamma_{m0}}$$

The lever arm (z) is equal to:

$$z = h_b - \bar{y}_{tee} \times 2$$

The area of the top or bottom tee-section is equal to:

$$A_{bt} = b_{fb}t_{fb} + \left(\frac{h_b - d_0}{2} - t_{fb}\right) \times t_{wb}$$

7.2 Yielding of Shear Tab in Rotation

The moment capacity of the fin plate can be calculated from its plastic section modulus and yield strength, using the equation below:

$$M_{pl,plate} = \frac{W_{pl}f_y}{\gamma_{M0}} \text{ (for short fin plate)}$$

Requirement for short fin plate:

$$\frac{t_p}{z_p} \geq 0.15 \text{ (P358, 2014)}$$

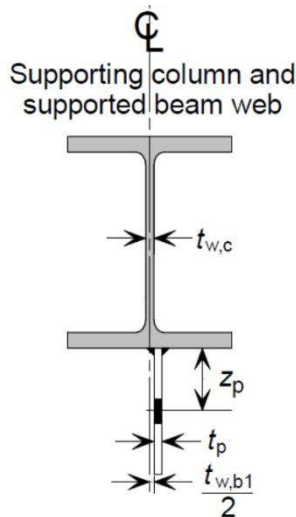


Figure 23: Setting out for a shear tab (SCI, 2014)

8 Concluding Remarks and Limitations

This FE study investigates the use of single standard and non-standard patented web openings in enhancing the ability of a RWS/WUF-B connection under monotonic and cyclic loading. An extended parametric study is performed by altering the opening depth, d_o , and the distance from the face of the column, S , for three different types of perforations, with 27 FE model connections developed and analysed. The following conclusions can be drawn:

- The variation of the opening depth, d_o , does the highest impact on the connection's strength and deformation, unlike the distance, S .
- RWS/WUF-B connections with perforated beams using small elliptically-based web openings ($d_o=0.5h$) do not experience a remarkable reduction in moment capacity, especially when the opening is positioned away from the column face ($S=700\text{mm}$).
- RWS/WUF-B connections using the non-standard web openings are found to be stronger and attain higher ultimate rotational capacities when compared to the traditional circular openings. Connections with web openings B are found to be the most optimum and controllable ones as a result of the narrow critical opening

length and small web opening area. Complimentary research suggests that the use of multiple and closely spaced openings B guarantees its light weight without compromising the web-post capacity of the beam between two adjacent web openings.

- The use of large openings ($d_o=0.8h$) is very effective in mobilising the plastic region away from the column face into the beam.
- On the other hand, the use of small openings led to the development of stresses on the face of the column, similar to the connections using solid webbed beams, which may extend around the top flange CJP weld. RWS/WUF-B connections with large openings located away from the columns face perform better minimising the stress concentration in the vicinity of the CJP welds.
- The use of large openings found effective in eliminating the panel zone shear deformations to the expense of lower maximum moment and rotational capacities. Medium size openings are ideal to reduce the interstory drift as well as maintain the ultimate connection capacities. In more detail, the optimal opening distance ($S=350\text{mm}$ or 520mm) is suggested.
- The maximum interstory drift recorded with the model using the smaller web opening B1 located at the largest distance, S , equal to 700mm (0.219radian) at peak strength and ultimate rotational capacity of 0.0499radian . This is a representative example, as the connection will fail by low-cycle fatigue fracture without local buckling within the reduced section similarly to the model with solid webbed beams.
- Previous researchers stated that the rotational capacities achieved by monotonic tests could be twice as high as the ones from cyclic tests. This is in agreement with the current findings in certain cases, as it can be seen from **Table 3**. In detail, for connections with medium and large size web openings located close to the face of the column the ratio of the monotonic over cyclic rotations is smaller or close to 1.0. The same ratio was found greater than 2.0 when small openings were used instead.
- All examined RWS/WUF-B connections using the new elliptically-based web openings have achieved the 0.05radian limit suggested by FEMA 356 (2000) for the RBS connections, as opposed to the RWS/WUF-B connections with circular openings. The acceptable criteria provided by the GSA and DoD specifications may

underestimate the rotational capacity that can be achieved by RWS/WUF-B connections.

- A step-by-step methodology for calculating the rotational moment capacity of RWB/WUF-B connections is presented. Comparing the estimates of the proposed design method, which is using information from FEMA 350 (2000), EC3 (2005) and P358 (2014), with the computational results presented in this paper, it is concluded that the proposed design method is satisfactory.

The results of this study suggest that the use of single large beam web openings can prevent excessive interstory drifts and reduce the stress intensity in the vicinity of the connection welds and bolts provided judicious use of the opening size, shape, and location. In this way, RWS/WUF-B moment connections with perforated beams can serve as a cheaper and a more feasible strengthening/weakening technique applied for code-deficient steel buildings. The use of the new elliptically-based web opening shapes A2 and B3 positioned at any distance, and most effectively at $S=350\text{mm}$ or 520mm from the column face, is proposed. This work sets provisional limits for the rotational capacities of such RWS/WUF-B connections and emphasises on the deviation of the results varying with the geometric parameters.

Acknowledgments

The first author of the paper would like to pass his thanks to his MEng students, Christopher Pilbin and Lau Chun Kit for the work they have conducted for the completion of this paper. Special thanks goes to the Institution of Structural Engineers (IStructE) for their financial support (Undergraduate Research Grants 2013/14) and the Innovation and Research Focus, UK (Issue 95, November 2013) promoting this research topic.

Notations

M_{pl}	Plastic moment capacity of reduced beam web section
$M_{pl,tt}$	Plastic moment capacity of top tee in reduced beam web section
$M_{pl,bt}$	Plastic moment capacity of bottom tee in reduced beam web section
$M_{pl,Rd}$	Plastic moment resistance of beam

$N_{bt,Rd}$	Tensile resistance of bottom tee
A_{bt}	Area of bottom tee in reduced beam web section
γ_{m0}	A factor equals to 1.0
f_y	Yield strength of steel
z	Lever arm
h_b	Height of beam
\bar{y}	Distance from centre of segments to elastic neutral axis
b_{fb}	Width of beam flange
t_{fb}	Thickness of beam flange
d_0	Web opening depth
d_c	Distance from plastic zone to column face
t_{wb}	Thickness of beam web
P	Applied point load at the center of beam
L'	Distance between the two web openings on each sides of the beam
W	Uniform distributed load on the beam
V_p	Shear at web opening
M_f	Moment at column face
x	Distance between web opening to column face
h_c	Column height
$V_{Rd,connection}$	Shear capacity of WUF-B connection
V_{Ed}	Design shear for WUF-B connection
$V_{Ed,G}$	Shear due to factored gravity load
$V_{Ed,S}$	Factored Shear due to seismic action
G	Unfactored permanent load
Q	Unfactored variable load
ψ_{2i}	Safety factor according to different types of buildings
L	Total length of beam
$V_{Ed,E}$	Unfactored shear due to seismic action
γ_w	Over-strength factor (i.e. $\gamma_w = 1.25$)
Ω	Minimum value of $\Omega = \frac{M_{pl,Rd}}{M_{Ed}}$ of all beams with dissipative elements (i.e. reduced beam web section)
$F_{v,Rd}$	Shear resistance of each bolt
A_S	Tensile stress area of each bolt
f_{ub}	Ultimate strength of bolt
α_v	A factor according to different class of bolts
h_{max}	Maximum depth of shear tab
$F_{b,Rd}$	Bearing capacity of each bolt
f_u	Ultimate strength of shear tab
$V_{wp,Ed}$	Design shear in column web panel zone
Z_{left}	The lever arm between the flanges of left beam
Z_{right}	The lever arm between the flanges of right beam
$M_{pl,Rd,left}$	Plastic moment resistance of left beam
$M_{pl,Rd,right}$	Plastic moment resistance of right beam
$V_{b,Rd}$	Shear resistance of column web panel zone
$V_{bw,Rd}$	The shear resistance of column web
$V_{bf,Rd}$	The shear resistance of column flanges

η	A value will be defined in National Annex. η equals to 1.2 for steel grades up to and include S460. For higher steel grades, the value is taken as 1.0
f_{yw}	Yield strength of column web
h_w	The height of column web
t_{wc}	Thickness of column web
γ_{M1}	A factor equals to 1.25
χ_w	Shear buckling factor
$\bar{\lambda}_w$	Modified slenderness
b_{cf}	Width of column flange
t_{cf}	Thickness of column flange
f_{yf}	Yield strength of column flange
c	A factor equals to $a \left(0.25 + \frac{1.6b_{cf}t_{cf}^2f_{yf}}{t_{cf}h_w^2f_{yw}} \right)$
a	Length of a stiffened or unstiffened plate
N_{Ed}	Axial force acting on column
A_{f1}, A_{f2}	Areas of column top flange and bottom flange
$M_{Rd,h}$	Moment resistance at column web
$M_{Ed,h}$	Design Moment at column web
$N_{stiffener,Rd}$	Tensile resistance of each stiffener plate
$A_{stiffener}$	Cross-sectional area of each stiffener plate
$\theta_{p,k}$	Rotation due to panel shear deformation
α	Ratio of effective depth of column to span length
β	Ratio of effective depth of beam to column height
V_c	Shear at column
θ_b	Rotational capacity of beam
$V_{eff,2,Rd}$	Block tearing resistance
A_{nt}	Tension area in net section fractures
A_{nv}	Shear area in net section fractures
$\theta_{connection}$	Rotational capacity of RWS/WUF-B ($\theta_{RWS/WUF-B}$)
$\theta_{plate\ yielding}$	The contribution of shear tab
$\theta_{bolt\ bearing}$	The rotation from the hole of the shear tab due to bolt bearing
$L_{plate\ yielding}$	The width of shear plate from column face to bolts
$I_{plate\ yielding}$	Second moment of shear plate
$w_{b,add}$	Additional deflection due to single web opening
w_b	Deflection of a beam without openings
l_0	Critical opening length ($l_0 = 0.45h_0$ for circular opening, $l_0 = 2R$ for elliptically opening)
h_0	Depth of openings
R	Radius of semi-circle in elliptical openings
w	Applied load at centre of the beam
l	Length of a beam
E	Elastic modulus

References

- Alashker, Y., Li, H. and El-Tawil, S. (2011) Approximations in Progressive Collapse Modeling. *Journal of Structural Engineering*, 137(9), pp. 914-924.
- ASCE/SEI 41-07. (2007) *Seismic Rehabilitation of Existing Buildings*. American Society of Civil Engineers, Reston, Virginia.
- Carino, N. and Lew. H.S. (2001) *Summary of NIST/GSA Workshop on Application of seismic rehabilitation technologies to mitigate blast-induced progressive collapse*. Proc., National Institute of Technology and Standards, Washington, D.C., No. NISTIR 6831.
- Department of Defense (DoD). (2005) *Unified Facilities Criteria (UFC) 4-023-03: Design of Buildings to Resist Progressive Collapse*, Washington, DC.
- Department of Defense (DoD). (2009) *Unified Facilities Criteria (UFC) 4-023-03: Design of Buildings to Resist Progressive Collapse*, U.S. Army Corps of Engineering, Washington, DC.
- Charney, F.A. and Downs W.M. (2004) Modeling Procedures for Panel Zone Deformations in Moment Resisting Frames. Proceedings of the Fifth International Workshop, Connections in Steel Structures V, Amsterdam, The Netherlands, June 3-4, 2004, pp. 121-130.
- EN1993-1-3 (2006) Design of Steel Structures - Part 1-3: General Rules - Supplementary rules for cold-formed members and sheeting, Brussels, Belgium.
- EN 1993-1-8 (2005): Design of Steel Structures - Part 8: Design of Joints, Brussels, Belgium.
- EN 1998-3 (2005) *Part 3: Design of Structures for Earthquake Resistance*. Assessment and Retrofitting of Buildings.
- FEMA 350 (2000). *Recommended Seismic Design Criteria for New Steel Moment-Frame Buildings, Chapter 3: Connection Qualification*, prepared for the SAC Joint Venture, published by the Federal Emergency Management Agency, American Society of Civil Engineers – ASCE, Washington, D.C.
- FEMA 356 (2000). *Prestandard and Commentary for the Seismic Rehabilitation of Buildings*, prepared for the SAC Joint Venture, published by the Federal Emergency Management Agency, American Society of Civil Engineers - ASCE, Washington, D.C.
- General Services Administration (GSA). (2003) *Progressive collapse analysis and design guidelines for New Federal Office buildings and major modernization projects*. The U.S. General Services Administration. Washington, DC.

- General Services Administration (GSA). (2008) *Progressive collapse analysis and design guidelines for New Federal Office buildings and major modernization projects*. The U.S. General Services Administration. Washington, DC.
- Hamburger, R. and Whittaker, S.E. (2004) Design of Steel Structures for Blast-Related Progressive Collapse Resistance. *The Steel Conference, Northern American Steel Construction Conference*.
- Hedayat, A.A. and Celikag, M. (2009) Post-Northridge connection with modified beam end configuration to enhance strength and ductility. *Journal of Constructional Steel Research*, 65(0), pp. 1413-1430.
- Kazemi, M. and Hosseinzadeh, A. (2011) Modelling of inelastic mixed hinge and its application in analysis of the frames with reduced beam section. *International Journal of Steel Structures*, 11(1), pp. 51–63.
- Khandelwal, K. and El-Tawil, S. (2007) Collapse behaviour of steel special moment resisting frame connections. *Journal of Structural Engineering*, 133(5), pp. 646-655.
- Kim, T. and Kim, J. (2009) Collapse analysis of steel moment frames with various seismic connections. *Journal of Constructional Steel Research*, 65(6), pp.1316-1322.
- Kim, T., Kim, U.S. and Kim, J. (2012) Collapse resistance of unreinforced steel moment connections. *The Structural Design of Tall and Special Buildings*, 21(10), pp.724-735.
- Kim, J. and Park, J. 2008. Design of Steel Moment Frames Considering Progressive Collapse. *Steel and Composite Structures*, 8(1), pp. 85-98.
- Mao, C., Ricles, J., Lu, L. and Fisher, J. (2001) Effect of Local Details on Ductility of Welded Moment Connections. *Journal of Structural Engineering*, 127(9), pp.1036-1044.
- P355 (2011) *Design of Composite Beams with Large Web Openings*, edn., United Kingdom: The Steel Construction Institute, The British Constructional Steelwork Association Limited.
- P358 (2014) *Joints in Steel Construction - Simple Joints to Eurocode 3*, edn., United Kingdom: The Steel Construction Institute, The British Constructional Steelwork Association Limited.
- Prinz, G.S. and Richards, P.W. (2009) Eccentrically braced frame links with reduced web sections. *Journal of Constructional Steel Research*, 65, pp. 1971–1978.
- Ricles, J.M., Mao, C., Lu, L.W. and Fisher, J.W. (2003) Ductile details for welded unreinforced moment connections subject to inelastic cyclic loading. *Engineering Structures*, 25(5), pp.667-680.

- Redwood, R. (1983) Design of I-Beams with Perforations, Beams and Beam Columns, Stability and Strength. Applied Science Publishers, London.
- Sadek, F., Main, J., Lew, H. and Bao, Y. (2011) Testing and Analysis of Steel and Concrete Beam-Column Assemblies under a Column Removal Scenario. *Journal of Structural Engineering*, 137(9), pp.881-892.
- Sofias, C.E., Kalfas, C.N. and Pachoumis, D.T. (2013) Experimental and FEM analysis of reduced beam section moment endplate connections under cyclic loading. *Engineering Structures*, 59, pp. 320-329.
- Steel Construction Institute (2014) '*Fin Plates*', in The Steel Construction Institute (ed.) Joints in Steel Construction - Simple Joints to Eurocode 3. United Kingdom: The Steel Construction Institute, The British Constructional Steelwork Association Limited., pp.109.
- Tsavdaridis, K.D. and D' Mello, C. (2011) Web Buckling Study of the Behaviour and Strength of Perforated Steel Beams with Different Novel Opening Shapes. *Journal of Constructional Steel Research*. 67(10), pp.1605-1620.
- Tsavdaridis, K.D. and D'Mello, C. (2012a) Optimisation of Novel Elliptically-Based Web Opening Shapes of Perforated Steel Beams. *Journal of Constructional Steel Research*, 76(0), pp.39-53.
- Tsavdaridis, K.D. and D'Mello, C. (2012b) Vierendeel Bending Study of Perforated Steel Beams with Various Novel Shapes of Web Openings, through Non-Linear Finite Element Analyses. *Journal of Structural Engineering (ASCE)*, 138(10), pp.1214-1230.
- Tsavdaridis, K.D. and D'Mello, C. FE Modelling Techniques for Web-Post Buckling Response: Perforated Steel Beams with Closely Spaced Web Openings of Various Shapes. *The 6th European Conference on Steel and Composite Structures (EUROSTEEL)*. 31 August - 2 September 2011, Budapest, Hungary, Reference no: A-0378, Vol. C, pp. 1851-1856.
- Tsavdaridis, K.D. (2014) *Strengthening Techniques: Code-deficient Steel Buildings, to the section: Structural Engineering-Structural Design*, Encyclopedia of Earthquake Engineering, pp. 1-26.
- Tsavdaridis, K.D., Faghih, F. and Nikitas, N. (2014) Assessment of Perforated Steel Beam-to-Column Connections Subjected to Cyclic Loading. *Journal of Earthquake Engineering*, 18(8), pp.1302-1325.

- Tsavdaridis, K.D. and Papadopoulos, T. (2016) A FE Parametric Study of RWS Beam-to-Column Bolted Connections with Cellular Beams. *Journal of Constructional Steel Research*, 116, pp.92-113.
- Yang, Q., Li, B., and Yang, N. (2009) Aseismic Behaviors of Steel Moment Resisting Frames with Opening in Beam Web. *Journal of Constructional Steel Research*, 65, pp. 1323-1336.